

**EFFECT OF TiC REINFORCEMENT ON WEAR RESISTANCE OF MAGNESIUM MATRIX COMPOSITE BY FSP**

In the current study, wear performance of pure magnesium (Mg) and composite fabricated with titanium carbide (TiC) reinforcement is investigated under various loading and sliding velocity conditions. The Mg-matrix composite is prepared by friction stir processing (FSP) carried out at optimized values of process parameters. Sliding wear tests on Mg and friction stir processed (FSPed) Mg+TiC surface composite were done on pin-on-disc configuration. The consequence of the normal load applied and sliding velocity on wear behaviour of the two materials is evaluated by performing the tests at two normal loads of 6 N and 12 N and three sliding speeds of 0.5 m/s, 1.5 m/s and 4.5 m/s. FSPed composite found to exhibit an enhanced wear resistance as compared to that of pure Mg. To get an insight into the possible types of mechanisms for wear of the composites sample under varying load and sliding speeds conditions, the worn test specimens are subjected to scanning electron microscopy (SEM). SEM/EDS analysis revealed that oxidation, ploughing, trailing edge and 3-body abrasive wear were the predominant mechanisms for the wear of samples at a different set of experimental conditions. The tensile strength of the FSPed surface composite was found to be 25% higher than pure Mg. Wear resistance was found to increase by about 33%.

*Keywords:* Friction stir processing; FSP; wear behavior; surface composites; Mg composites; TiC composite

**1. Introduction**

A higher value of specific strength in magnesium and its alloys makes them a suitable for a wide range of popularity in the aerospace and automotive sector in addition to the electronic industry. However, having a single material with all the tribological and mechanical properties together is very difficult. Consequently, time demands to get a way to make better-quality products with a mix of two or more desirable properties. [1]. The high specific strength directly correlates to weight reduction and hence provides an economic advantage. However, poor surface properties and casting defects like porosity limit the extent to which Mg and Mg-alloys can be used in such applications [2]. Apart from the improvement in mechanical properties and corrosion resistance; tribological properties, like wear and friction are the fundamental requirements of a successful engineering design [3]. Mixing of two different elements to produce a composite and refinement of grain plays a significant role in enhancing the tribological and mechanical properties together. There are various ways to fabricate a composite material like Stir casting, Powder metallurgy and squeeze casting used conventionally [4].

FSP is the recent, effective, simple and widely used severe plastic deformation (SPD) technique in improving the tribological performance of engineering materials [5] and hence is selected for the present work. Mishra et al. [6] fabricated Aluminum matrix Silicon Carbide in the previous decade opening a gateway to new composite fabrication process. The thickness of the fabricated surface composite layer was found to be in the range of 50 to 200  $\mu\text{m}$ . The microhardness was found to be 173 HV nearly double of the 5083Al alloy matrix which was 85 HV before processing.

The wear behavior in dry sliding conditions of two different Mg-alloys is studied by An et al [7] wherein,  $\text{Mg}_{97}\text{-Zn}_1\text{-Y}_2$  alloy exhibited superior resistance to wear in comparison to the AZ91 alloy at a load and sliding velocity of 80 N and 0.785 m/s respectively. Block-on-wheel system was used by Zhang et al [8] to look at the performance of the as-cast Mg-Zn-Y alloy under load settings in the range of 10 to 70 N. It was observed superior performance of this alloy at the value of sliding speed as 0.42 m/s with a range of the time from 10 to 40 min. Some investigations for evaluation of the tribological behavior of Mg-based composites have also been done by the researchers.

<sup>1</sup> I.K. GUJRAL PUNJAB TECHNICAL UNIVERSITY, DEPARTMENT OF RESEARCH, INNOVATION AND CONSULTANCY, PUNJAB, INDIA

<sup>2</sup> MECHANICAL ENGINEERING DEPARTMENT, BEANT COLLEGE OF ENGINEERING AND TECHNOLOGY, PUNJAB, INDIA

<sup>3</sup> MECHANICAL ENGINEERING DEPARTMENT, THAPAR INSTITUTE OF ENGINEERING AND TECHNOLOGY, PUNJAB, INDIA

\* Corresponding author: balraj1507@gmail.com



The addition of  $\text{Al}_2\text{O}_3$  nano-particles helped to increase the wear resistance of pure magnesium and AZ31 matrix alloy [9] owing to increased work-hardening. Mechanism of wear of ZE41A-Mg alloy at variable sliding velocities was studied by López et al. [10]. Oxidation was observed the principal wear mechanism at the low sliding velocity 0.1 m/s. Whereas, at intermediate and higher sliding speeds, abrasion and delamination are the fundamental causes of wear under intermediate loads.

However, attainment of feasibility and improvement in the rate of production, several control parameters are needed to be optimized in FSP. Tool shape, tool dimensions, tool rotating and linear speed, plunge depth and axial force applied were some of the important parameters that affected the microstructural grain refinement in FSP. Arora et al. [11] concluded that apart from other factors, the microstructural evolution was found to be a function of cooling condition and the number of passes. Aathisugan et al. [12] fabricated graphite and boron carbide reinforced Mg-alloy (AZ91D) based hybrid composite using FSP. Results revealed an increased wear resistance of hybrid composites compared with AZ91D alloy due to hardness but at the cost of decreased ultimate tensile strength. Tinubu et al. [13] evaluated the mechanical and wear performance of precipitation-hardened alloy of A-286 stainless steel after FSP. Wear resistance was found to improve from  $1 \times 10^{-6} \text{ mm}^3/\text{Nm}$  to  $6 \times 10^{-7} \text{ mm}^3/\text{Nm}$  with increasing micro-hardness of nugget zone which was attributed to the grain refinement resulting from the Hall-Petch strengthening mechanism.

Huang et al. [14] applied stirring casting along with FSP to fabricate Mg-6Zn composites. The grain refinement and load transfer in addition to Orowan looping mechanisms contributed to improve strengthening. Singh et al. [15] used B4C reinforcement to fabricate AZ91 based composite with FSP under natural cooling to get improved wear resistance and microhardness apart from grain refinement of AZ91. The microhardness and wear resistance was found to be improved for the composite at a sliding velocity of 1m/s and 5 N normal load. Arokiasamy et al. [16] have investigated the improvement in the mechanical behaviour of surface composites produced by stir casting with Mg-matrix and SiC and  $\text{Al}_2\text{O}_3$  as reinforcement. FSP was done at three tool rpm levels and three levels of tool feed and microstructural studies revealed that the grain size got refined from 84 to 7  $\mu\text{m}$ . Process parameters were also optimised to get the finest grain size accompanied by improved hardness, tensile strength and wear resistance. Dadashpour et al. [17] examined the effect of FSP parameters and addition of  $\text{SiO}_2$  nano powder on the mechanical behaviour and the fracture strength. The results showed that the mechanical properties of composites were improved than the base metal and fine grains were obtained. The hardness and the strength of the nanocomposites was also increased. However, the fracture strength was found to be deteriorated with FSP. Azizieh et al. [18] fabricated in-situ pure Mg-matrix surface nanocomposites with Al particles using FSP. Microstructural analysis revealed a grain refinement due to dynamic recrystallization. SEM and XRD confirmed that formation of  $\text{Al}_{12}\text{Mg}_{17}$  inter metallics during FSP which was attributed to the chemical

reaction at the Al-Mg interface. Najafi et al. [19] found the grain size of 800 nm in SiC reinforced Mg alloy AZ31-matrix surface composite produced by single pass of FSP using methanol mixed with dry ice and achieved the grain size of 1 nm.

From the detailed literature survey, it was observed that a plenty of work has been done to fabricate composite using alloys of Magnesium. However, study of pure Mg based composite by FSP was found to be almost missing and effect of composite fabrication on mechanical and tribological properties was meagrely studied. In the current investigation, an effort is made to investigate the improvement in the wear resistance along with mechanical properties of pure magnesium (Mg) matrix composite using TiC particles by FSP. Optimized FSP control parameters are used to prepare the TiC particle reinforced surface Mg composite. Afterwards, pure Mg and FSPed Mg+TiC composite samples are subjected to tensile and wear testing to evaluate their mechanical and wear properties. X-ray diffraction (XRD) and scanning electron microscopy (SEM) are applied to examine the surface of test specimens before and after carrying out the tests.

## 2. Experimental details

### 2.1. Material preparation

Rectangular specimens having 80 mm length, 40 mm width and 4 mm thickness are prepared from Commercial purity Magnesium (99.9%), block using wire cut EDM. The surface is then polished using emery up to 2000 grit size. Holes (1 mm diameter, 1.2 mm depth and 5 mm pitch) are drilled in polished rectangular blocks by mounting them in a specially fabricated fixture as shown in Fig. 1. After drilling, the holes are filled with Titanium Carbide (TiC) powder at 325 mesh which refers to a particle size of 45  $\mu\text{m}$ . The surface composites were prepared on a 5 H.P. computer numeric controlled (CNC) vertical milling machine (VMC) mounted with exclusively fabricated FSP fixture as discussed. A cylindrical stainless steel FSP tool having shoulder dia as 16 mm, pin dia as 3 mm and length of the pin as 1.6 mm has been used to perform the experiments.

The controlling parameters optimized used in the study are: tool rpm = 600 rpm, plunge depth = 0.35 mm, under surface cooling temperature  $-10^\circ\text{C}$ , three passes of FSP tool at a linear speed of 15 mm/s. The fixture consists of a hollow rectangular box-like configuration to enable the flow of cooling liquid under the specimen surface and assist in cooling of the specimen. To achieve rapid cooling of FSPed specimens, a 250 Watt cryostat cooling bath having eight-liter capacity is used with reagent (LR) grade refrigerant as the working fluid. Polyurethane (PU) pipes connected to the cryostat chiller unit carry the coolant (Methanol) to the fixture. The standard metallographic technique is followed for preparing the surface of test specimens at an etching time of 30 s with a solution mixture of 6 gm picric acid, 5 ml acetic acid, 100 ml ethanol and 10 ml water.

The microstructural examination of the as-cast and worn specimens of pure Mg and FSPed Mg+TiC composites is ac-



Fig. 1. Actual set-up on CNC vertical milling machine

completed on a scanning electron microscope (JSM-6610LV, JEOL, Japan) and X-ray diffractometer (PANalytical X'Pert Pro, Netherlands).

## 2.2. Micro-Hardness Test

Micro-hardness was the primary mechanical property considered for evaluation of tribological behaviour improvement. The micro-hardness testing of the FSPed composites was carried out on a Vickers Tester (Model 402 MVD) and Wilson Instruments make. The micro-hardness measurements were taken at ten different places on the polished surfaces and their average value was taken as the micro-hardness (HV) of the specimen. The testing of micro-hardness was accomplished at 0.5 kgf load for a period of dwell of 10 seconds.

## 2.3. Tensile Test

Mechanical properties of the pure Mg as well as the fabricated composite were determined using micro-hardness and tensile tests. Microhardness test was performed on Microhardness Tester Wilson (Instron) [Model401/402MVD] at 500gf load for a dwell period of 10s. Mini-tensile specimens having a gauge length of 10 mm, width 4 mm and thickness 3 mm were prepared from as-cast pure Mg and fabricated surface composite specimens. Tensile properties including 0.2% yield strength, ultimate tensile strength, elongation to failure and strain hardening exponent were obtained. The difference in microhardness along the horizontal below nugget zone and cross-section were determined for the fabricated composite. The tensile strength of pure Mg and FSPed Mg+TiC surface composite is explored by carrying out a tensile test on a universal testing machine (Tinius Olsen, United Kingdom) at a strain rate of  $10^{-3}$ .

## 2.4. Wear Test

The wear performance of the pure Mg and TiC-particle reinforced composites is evaluated by performing wear tests on square-pin test specimens. The pin specimens (side = 6 mm and thickness = 3.5 mm) are machined from the as-received pure Mg and FSPed Mg+TiC composite using wire-EDM (electrical discharge machining). Sliding wear test in the dry condition is then performed on the cut samples using a universal tribometer (CETR UMT3, USA). The tribometer consists of a pin-on-disc arrangement with a facing plate made of SS 316 grade having an approximate hardness of 220 HV. The wear test is performed for 1500 m sliding distance at sliding speeds of 0.5, 1.5 and 4.5 m/s under two vertical loads of 6 and 12 N. To prevent contamination and ensure accuracy of the results, the disc, and the test specimens are cleaned after each test using acetone followed by air drying. The loss of weight as a function of distance traveled by the pin in sliding is determined up to an accuracy of 0.01 mg. Keeping the test parameters constant, all the tests are repeated twice to get reliable data. Possible wear mechanisms were analysed with SEM/EDS analysis.

## 3. Results and discussion

### 3.1. Microstructural analysis

Fig. 2 shows the XRD peak pattern with the characteristics and elemental composition of the samples. For both the samples considered in this study, the value of  $2\theta$  varies from  $10-100^\circ$ . It is observed from Fig. 2(a) that as-cast Mg exhibits the major phases of Mg only. The XRD examination of the FSPed Mg-based surface composite reinforced with TiC particles as shown Fig. 2(b), depicts the different phases of TiC along with the major peaks of Mg and TiC. Larger peaks show the presence of the  $Mg_2TiO_4$  phase in the FSPed composite sample. TiC is seen along with the oxides of Mg and Ti indicating the mixing of reinforcement in the matrix material. This fine particles along with the refine Mg grains added to the microhardness which in turn improved the wear resistance of the composite. TiC powder reacts with Mg-matrix to form a uniformly dispersed phase. Rapid cooling just after the completion of the FSP may have contributed to grain refinement. The presence of oxides of Mg and Ti is the indication of mixing of TiC reinforcement in Mg matrix. Similar results have been quoted by Singh et al. [15], where Mg based alloy AZ91 was processed by adding  $B_4C$  to fabricate a surface composite.

Fig. 3(a) represents the SEM image of the TiC powder used in the study and SEM micrograph of the fabricated surface composite is shown in Fig. 3(b). TiC particles can be clearly seen in the given SEM micrograph in Fig. 3(b). Also the image represents the refinement of grains of substrate metal i.e. pure Mg.

Microstructure of the fabricated composite has been represented in the Fig. 4 whereas Fig. 4(a) represents the nugget zone where the FSP has been carried out to fabricate the surface com-

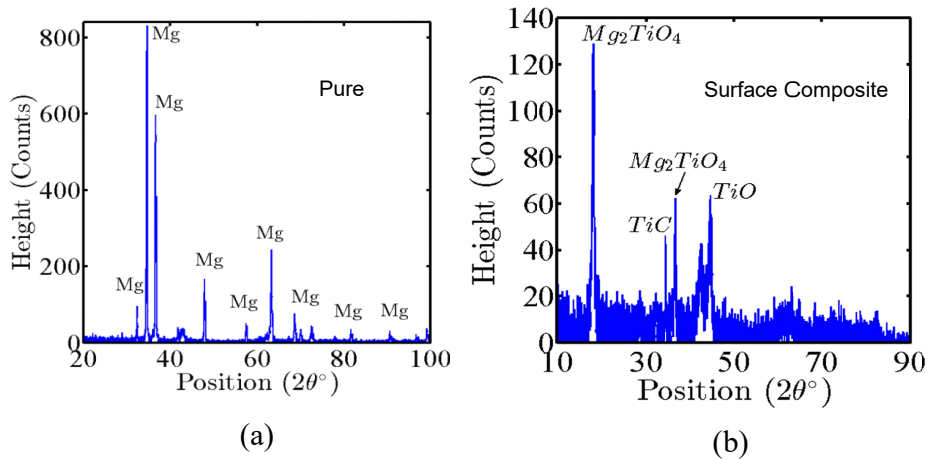


Fig. 2. X-Ray Diffraction peak pattern of: (a) pure Mg and (b) Mg+TiC composite fabricated by FSP

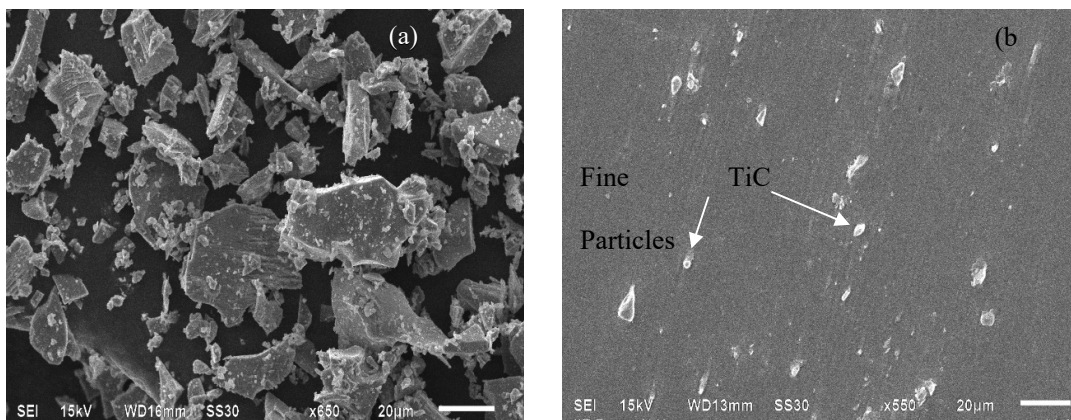


Fig. 3. SEM micrograph of (a) TiC powder and (b) Surface fabricated surface composite by FSP

posite. Fig. 4(b) presents the unprocessed zone wherein no effect of heat has been experienced by the specimen and in Fig. 4(c) heat affected transition zone is shown. In this zone, effect localized heat of the FSP tool can be seen. Together processed zone and transition zone comprise the heat affected zone (HAZ). As friction under the action of axial thrust produces heat and the FSP tool exerts huge pressure just below tool pin which results in refined grains.

### 3.1. Micro-hardness test

Microhardness test has been conducted at a load of 0.5 kgf and the result revealed that the micro-hardness was found to increase from nearly 38 HV to about 62.4 HV exhibiting an improvement of about 63%. Fig. 5 represents the the micro-hardness measurement of the fabricated specimen across the cross-section.

### 3.2. Tensile strength

The output of the tensile test performed on pure Mg and FSPed Mg+TiC composite obtained in the form of the graph

between true stress-strain is represented in Fig. 6. Both the test materials represent quasi-linear elastic deformation. Pure Mg shows linear elasticity up to 40 MPa, Mg+TiC composite is linearly elastic up to a slightly lower value of about 32 MPa. As soon as the elastic limit is crossed, both the materials show plastic deformation (Fig. 6). It is quite evident from Fig. 6 that the surface composite has higher yield strength (by 33%) and ultimate strength (by 20%) than pure Mg. Table 1 represents the characteristics of the tensile behaviour exhibited by the pure Mg and TiC-Mg composite. One of the possible reasons behind the observed improvements in ultimate strength and yield strength of pure Mg is the microstructural refinement offered by severe plastic deformation occurred during FSP and the addition of TiC particles. Hence, the addition of hard particles of TiC helps in modifying the mechanical properties of the base material Mg by increasing the tensile strength with a corresponding decrease in elasticity. The grain refinement offered by the TiC-particles in FSP fabricated surface composite further improves the modulus of the processed composite.

However, the higher strength of FSPed Mg+TiC composite is compromised with a ~27% loss in ductility as compared to pure Mg. Pure Mg shows delayed necking phenomenon up to about 14.5% strain, compared to the 10% strain in Mg matrix surface composite. Moreover, after the commencement of necking for-

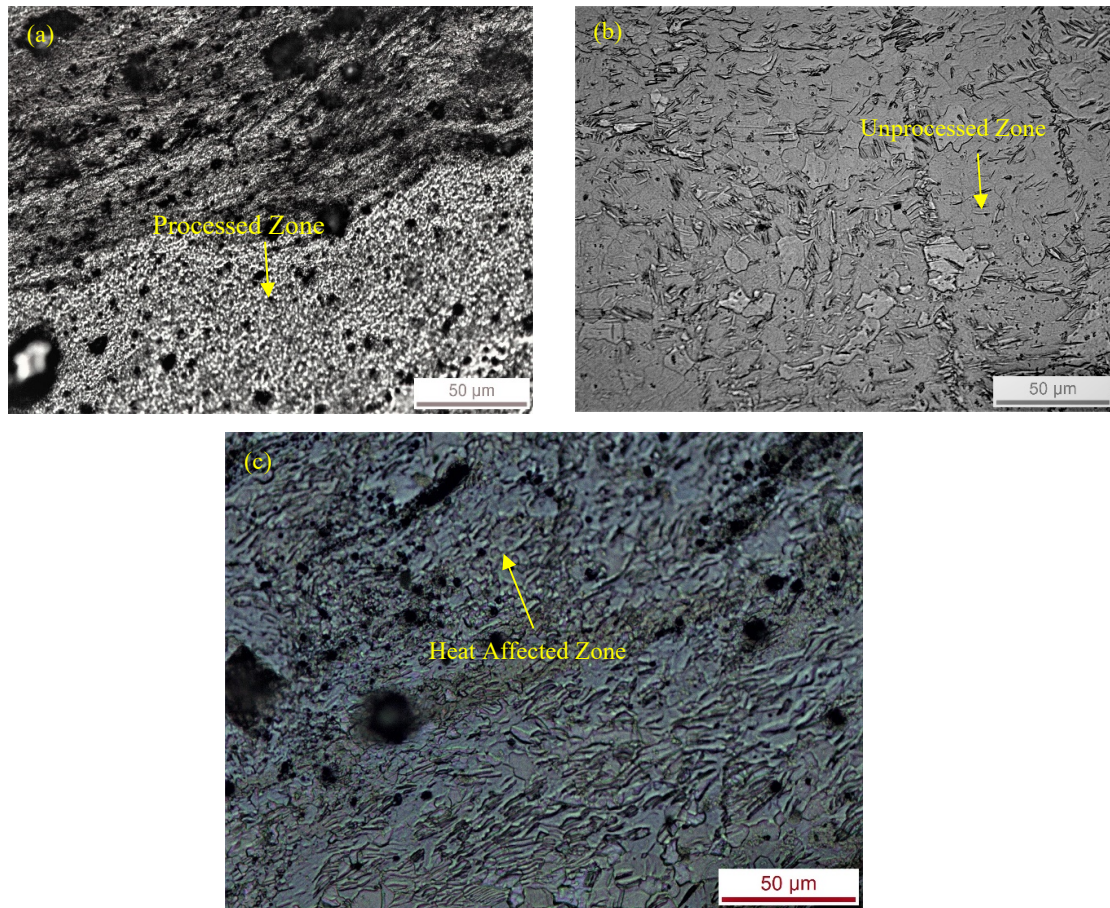


Fig. 4. Micrographs of fabricated Mg-based composite, a) Nugget (Processed) Zone, b) Unprocessed Zone and c) Transition Zone by FSP at optimized parameters

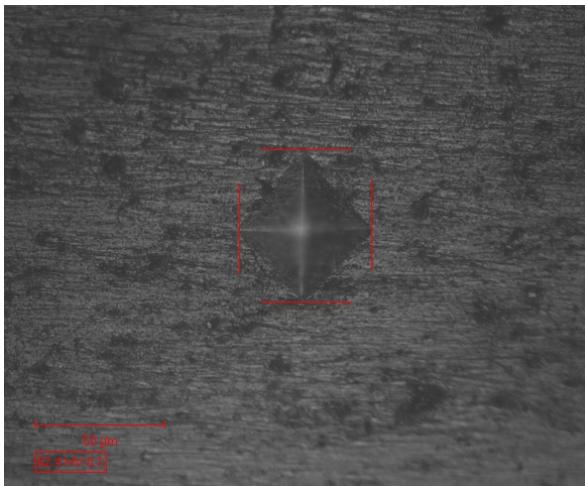


Fig. 5. Micrograph showing the microhardness of the fabricated specimen across the cross-section

mation, pure Mg shows a ductile failure by failing after nearly 18.8% elongation than the 13.7% failure strain in the surface composite. Similar results have been quoted by Aror et al. [20] for processed AE 42 Mg alloy. This loss in ductility of the FSPed surface surface composite may be linked to the work hardening of the material under the high pressures of friction stir processing.

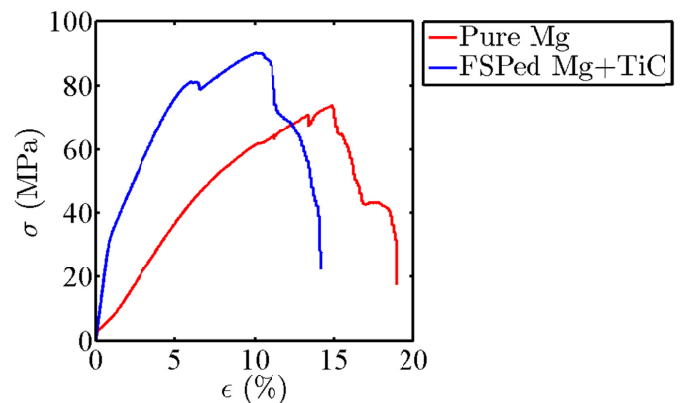


Fig. 6. Stress ( $\sigma$ ) versus strain ( $\epsilon$ ) plot obtained from the tensile testing of pure Mg and Mg+TiC composite fabricated by FSP

TABLE 1

Mechanical properties for the pure Mg and FSPed TiC-Mg Composite obtained from tensile test performed at 1 103 s<sup>-1</sup> strain rate

Sr.	Material no.	YS (MPa)	UTS (MPa)	Elongation (%)	Young's modulus (MPa)	Strain hardening exponent
1	Pure Mg	65±10	65±10	15±0.5	20	0.75
2	TiC-Mg Composite	90±10	90±10	10±0.5	25	0.50

### 3.3. Wear test

#### 3.3.1. Wear behaviour

Getting some positive insights from the tensile tests, the performance of pure Mg and its surface composite during wear testing is assessed next. The deviation in the rate of wear for as-cast pure Mg and FSPed surface composite with sliding distance as a function of applied speed and normal load is presented in Fig. 7. It is observed that the FSPed composite exhibits improved wear resistance at all the loading and velocity conditions. The wear rate curve is smooth for the FSPed composites. Furthermore, uniform wear rates have been shown for both as-cast pure Mg as well as FSPed composite over a large range of sliding distance at most of the loadings. It is found that at all sliding velocities varying between 0.5-4.5 m/s and under both the normal loads of 6 N and 12 N, the FSPed Surface composite shows a lower wear rate and hence higher wear resistance as compared to pure Mg. Thus, it can be established that the overall wear resistance of Surface composite fabricated by FSP is better than that of pure Mg. Arora et al. [2] have reported similar results during wear test for FSPed Mg-alloy AE42 at various normal loads ranging between 5-20 N and variation in velocities from 0.33-3 m/s. Singh et al. [15], fabricated a surface composite of Mg based alloy AZ91 with  $B_4C$  reinforcement and reported the improvement in wear resistance.

On critical examination of the plots in Fig. 7, one can see the decline in the rate of wear with the rise in sliding velocity at all the load values. Also, the wear resistance of both the materials considered in this study is improved with a decrease in applied normal load at a particular sliding velocity. Still, TiC reinforced Mg composites fabricated using FSP show better wear performance than pure Mg. This fact supports the dominance of different mechanisms of wear at dissimilar sliding speeds and loading conditions, which becomes clear from Fig. 7 as discussed in the next section.

Fig. 8(a) represents the variation in the rate of wear versus sliding speed under different loading conditions for pure Mg as well as Surface composite. It is observed that maximum wear occurs at the slowest speed of 0.5 m/s, and the rate of wear reduces with the rise in the value of sliding velocity for both the tested samples at all loads considered. Further, the wear rate of pure Mg at the highest value of wear velocity of 4.5 m/s under applied loads of 3 and 12 N is nearly similar to that of Surface composite. This implies that at higher sliding velocities pure Mg shows a wear resistance that is at par with that of TiC-particle reinforced FSPed composite. Whereas, at slower sliding velocities the surface surface composite shows far better wear rate than pure Mg. Fig. 8(b) represents the distinction in the rate of wear and normal load for pure Mg and FSPed Surface composite samples at variable sliding velocities. It can be concluded from the plot that the rate of wear augmented with the

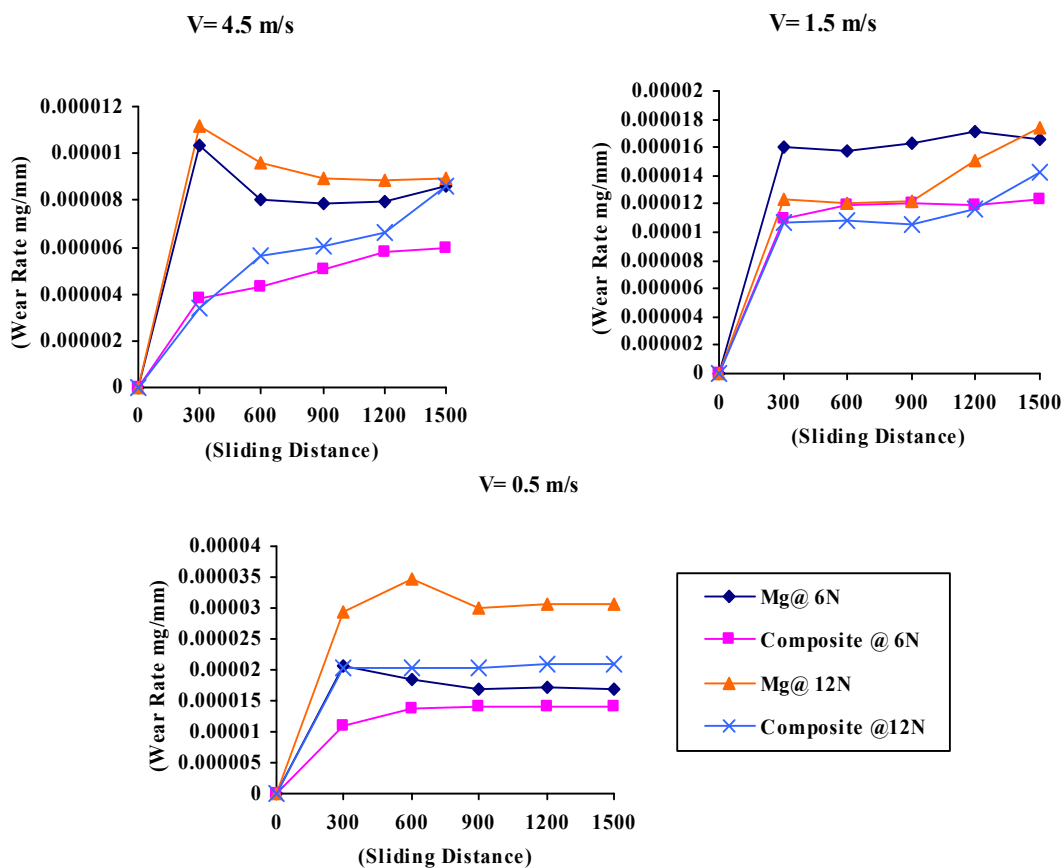


Fig. 7. Plot showing the rate of wear of pure mg and the fabricated composite at different sliding velocity under loading conditions and Common legend is given separately

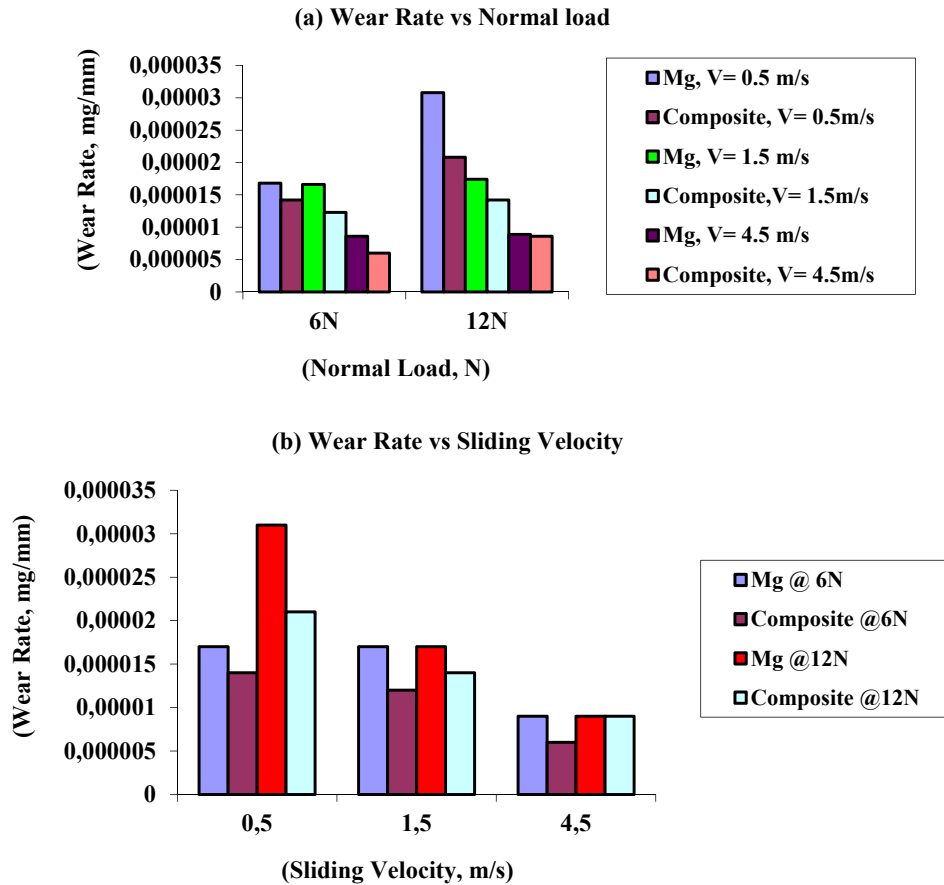


Fig. 8. Graphs between the (a) Rate of wear and Normal Load and (b) Rate of wear and Sliding velocity, for pure Mg and FSPed composite

load and is maximum at the highest value of load as 12 N and lower value of speed as 0.5 m/s. On the basis of result analysis of wear, the general trend for the variation in the rate of wear as a function of load and sliding velocity is summarized in Fig. 9. Hence, the minimum rate of wear can be achieved in Mg under the condition of the smallest value of the applied load and the highest value of sliding speed. The rate of wear can be further reduced by reinforcing pure Mg with TiC particles using FSP.

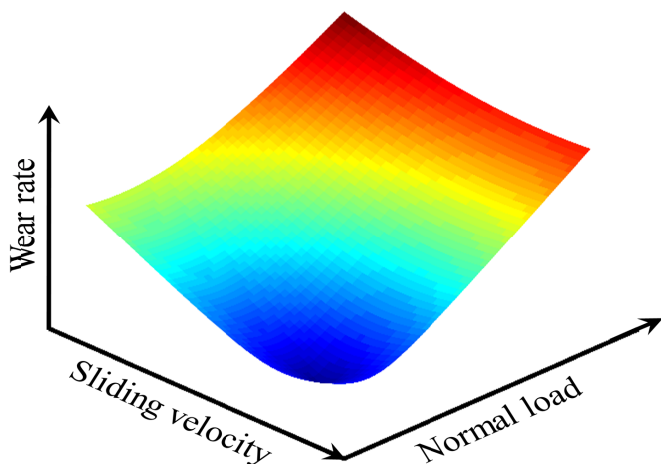


Fig. 9. 3-D Surface plot showing the rate of wear as a function of sliding speed and applied normal load

### 3.3.2. SEM/EDS Analysis Of Worn Out Samples

Fig. 10(a) represents the SEM image of the as-cast Mg and Fig. 10(b) represents EDS spectrum of worn out samples of unprocessed pure Mg from where after wear consists of Magnesium, Oxide of mg and small traces of carbon were observed. EDS spectrum confirms the the presence the presence of Mg and C particles on the surface of wron out pure Mg samples as shown in Fig. 10(a). SEM micrograph also represent the deep groove for this sample. The presence of Titanium Carbide particles added in Mg matrix enhanced its microhardness and wear resistance is confirmed in Fig. 10(b). EDS analysis of composite after wear test confirms the presence of Ti, C, O2 and Mg.

#### 3.3.2.1. At 6 N load

The predominant wear mechanisms at 6 N in FSPed surface composite are shown in Fig. 11(a) and (b). At a normal load of 6 N, different characteristics in the form of micro-cutting and continuous grooves are observed on the worn surface of the samples. These features of wear are an indicator of the abrasive wear along with oxidation at lower load value. Whereas, mechanism of wear changes with the rise in sliding speed from oxidation as seen in Fig. 11(a) to ploughing shown in Fig.11(b). In addition to these mechanisms, traces of delamination are also

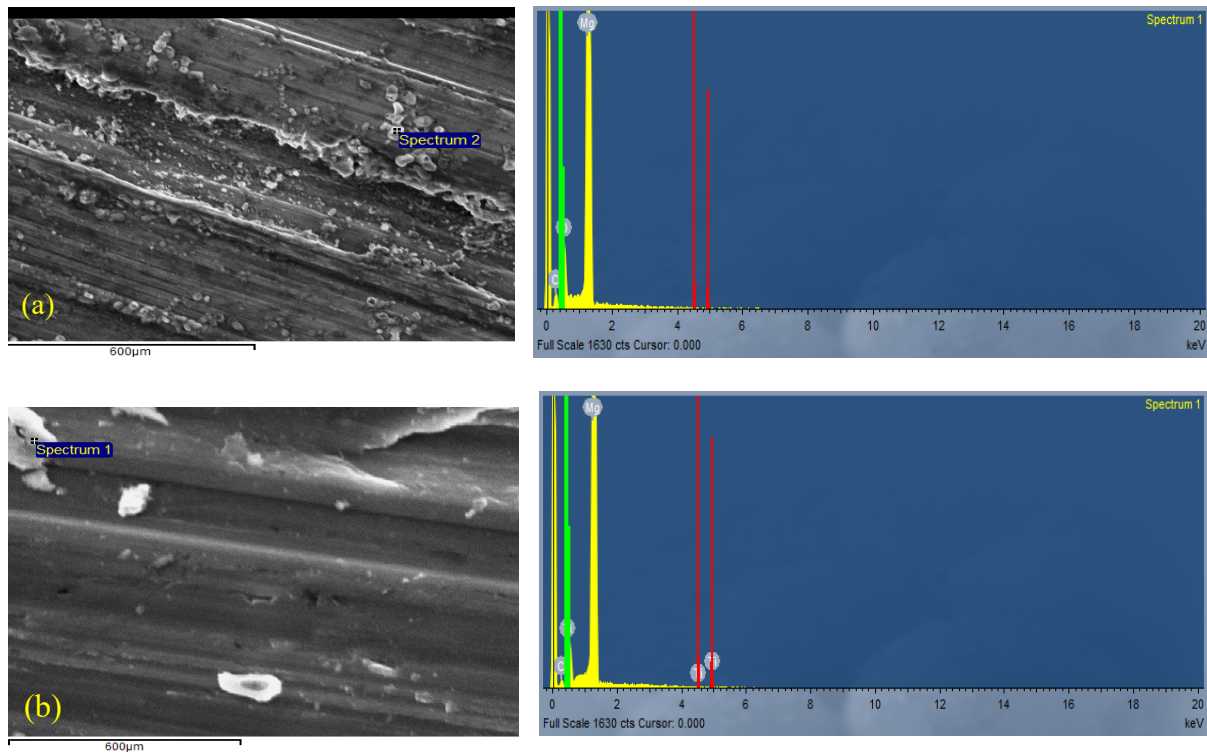


Fig. 10. EDS graphs of worn out a) pure Mg sample and b) TiC reinforced composite

visible at lower load value. Whereas at higher sliding speed above 1.5 m/s, the effect of delamination aggregate as of rise in subsurface cracks. The intensity of the abrasive wear increases with an increase in applied load. At lower sliding velocity, oxidation is the dominating wear mechanism, which is verified by the findings of López et al. [10]. However, at intermediate sliding velocities, trailing edge and ploughing come into the picture. On increasing the sliding velocity further to 4.5 m/s, abrasive wear becomes the predominant mode of wear. Therefore, the wear mechanism shifts from oxidation to the trailing edge and ploughing, and further to abrasive wear with an increase in sliding velocity.

### 3.3.2.2. At 12 N load

At 12 N load and 0.5 m/s sliding speed value temperature produced in the contact region between pin and disc witness a rise resulting in plastically deformed rolled edges. This plastic deformation occurred in FSPed composite only. This may be accredited to the improved ductility of the composite in comparison to the pure Mg, which has been ascertained by tensile test; similar behaviour has been reported by Arora et al. [20].

Oxidations gradually transformed to delamination of the surface under 12 N load at 1.5 m/s and 4.5 m/s as seen in Fig. 11(c). At highest velocity of 4.5 m/s, 3-body abrasive wear as represented in Fig. 11(d) at comparatively higher sliding velocities came into existence. The EDS analysis of the worn surface also supported smaller surface oxidation under these conditions. High shear force which is attributed to high normal

load and sliding velocity may have resulted in broken oxide layer on the worn surface. The presence of TiC particle during dynamic recrystallization of the matrix material may have restricted the growth of recrystallized nuclei. Restriction in growth of nuclei may result in finer grain structure in FSPed composite. So refinement in grain structure may be the responsible phenomenon for improved properties of the FSPed composite.

At higher load and sliding speed value temperature produced in the contact region between pin and disc witness a rise. A temperature rise decreases the yield strength of the material and led to the softening of the matrix. At higher load value this softened matrix deforms plastically. The effect of plastic deformation was not very dominating in the case of FSPed composite. The decrease in ductility of the FSPed sample may have attributed in the reduction of plastic deformation in it. The presence of TiC particle during dynamic recrystallization of the matrix material may have restricted the growth of recrystallized nuclei. Restriction in growth of nuclei may result in finer grain structure in FSPed composite. So refinement in grain structure may be the responsible phenomenon for improved properties of the FSPed composite. Fig. 12 represents the conversion of wear mechanisms with respect to the increase in sliding velocity. As the velocity increases, the wear mechanisms shift from oxidation to trailing edge, ploughing and abrasive wear.

### 3.3.3. Work Hardening

Plastic deformation of subsurface also contributes towards work hardening of the layers of subsurface considerably affecting

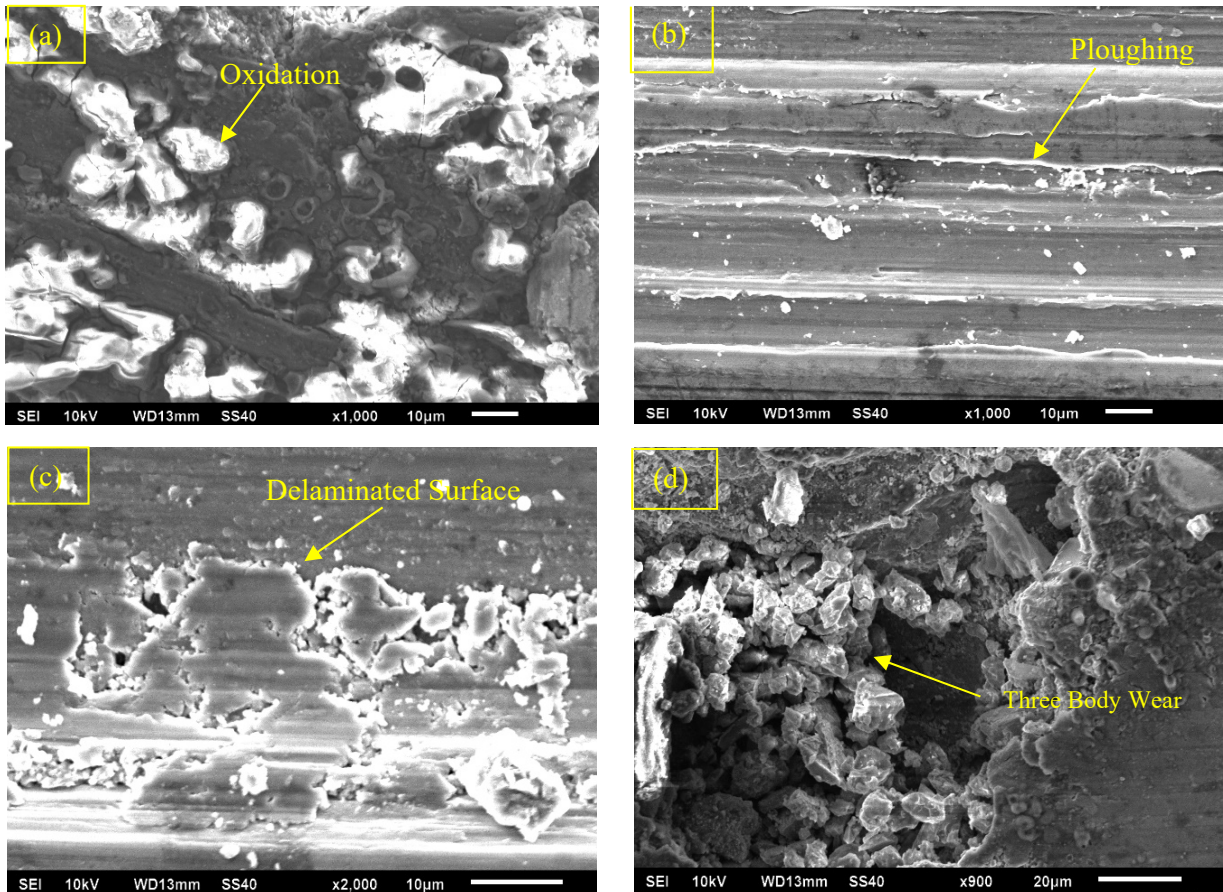


Fig. 11. Different wear mechanisms in FSPed Surface surface composite: (a) Oxidation at 6 N, (b) trailing edge at 6 N, (c) ploughing at 12 N and (d) 3-body at 12 N, after wear

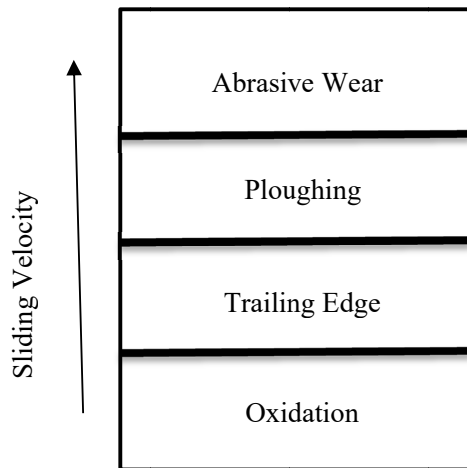


Fig. 12. Conversion of wear Mechanisms with the increase in sliding velocity

the wear characteristics of a specimen. To acquire a quantitative idea about subsurface work hardening effect, the microhardness of these subsurface layers of pure Mg as well as fabricated composite was examined, as shown in Fig. 13. Plot in the figure represents microhardness at 12 N load. It is obvious from the figure that the subsurface of both the pure Mg as well as fabricated surface composite got substantially work hardened. The

pure Mg subsurface shows maximum microhardness at 12 N load of nearly 60.1 HV, 68.2 and 74.6 HV at velocities of 0.5 m/s, 1.5 m/s and 4.5 m/s respectively. Values of microhardness for the FSPed surface composite is 105.1 HV, 113.5 HV and 118.6 HV respectively at velocities of 0.5 m/s, 1.5 m/s and 4.5 m/s. Arora et al. [20] also observed the phenomenon of work hardening due to wear at higher speeds and found wear resistance to improve. Further, it is noteworthy that at 12 N, the magnitude of work hardening of the material is higher at a lower sliding velocity

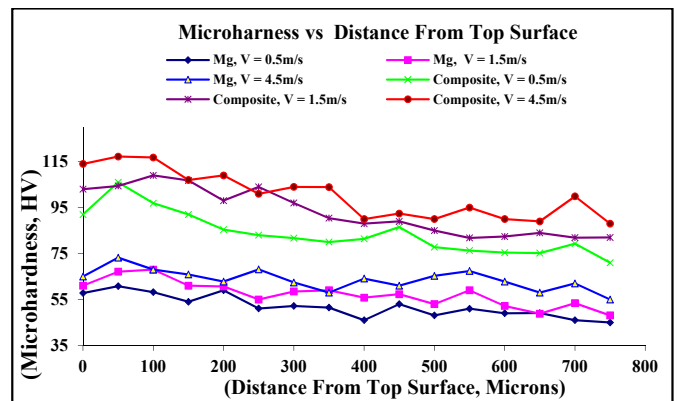


Fig. 13. Variation of microhardness of the wear tested specimens of pure Mg and surface composite at 12 N load

of 0.5 m/s than at 4.5 m/s even though, the material witnesses a higher strain rate at the increased velocity. Net mass loss decreases with the increase in velocity. Maximum reduction in cumulative wear has been observed at 6 N load which may be attributed to the higher heat generated due to friction between the pin and the disc.

This may be attributed to the higher quantity of heat produced on the surface of specimen at higher sliding velocity which resulted in elevated surface temperatures. At a normal load of 12 N maximum improvement in wear resistance has been recorded at lowest velocity which decreased at higher velocities. Besides, as is clear from the given chart the maximum work hardening occurs at locations lying 50-200 microns beneath the top surface.

#### 4. Conclusion

Wear behavior of pure Mg and TiC particle reinforced Mg composite is examined under various loading conditions and sliding velocities. The Mg surface composite is prepared by FSP of TiC particles on the surface of pure Mg. FSP is carried out at optimized parameters. Sliding wear test is carried out on pure Mg and its composite using a pin-on-disc setup in a universal Tribometer apparatus. Wear test is conducted at three normal loads of 6 N and 12 N along with varying sliding speeds of 0.5, 1.5 and 4.5 m/s.

- FSPed Surface composites were successfully fabricated with pure Mg as the matrix.
- FSPed TiC reinforced surface composites show an enhanced microhardness from 38HV to about 62.4 HV showing an improvement of about 63% and hence, improved the wear resistance than pure Mg.
- The rate of wear is found to decline by decreasing the applied normal load and with increasing sliding speed. Also, the wear mechanism is found to shift from oxidation to trailing edge and ploughing and further to abrasive wear on the increase in sliding velocity.
- A maximum wear resistance improvement of 33% has been observed at a normal load of 12 N and velocity of 0.5 m/s. However, a maximum of 30% reduction in net wear has been noticed at highest velocity i.e 4.5 m/s.
- The tensile behavior of both materials is also evaluated. With an approximate elongation of 18.8%, pure Mg proves to be more ductile than the composite. However, the FSPed Mg+TiC surface composite has an ultimate strength of nearly 20% higher than pure Mg.

Hence, the microstructural refinement due to the incorporation of TiC-particles in pure Mg-matrix improves the tensile strength, tensile modulus as well as the wear behavior of the fabricated composite. Low normal load and high sliding speed are found to be the best performance parameters to have the least wear rate. From the experimental output, it is found that at a sliding velocity of 4.5 m/s and a normal load of 6 N and results in the least wear of Mg and its composite.

#### Future Scope

The research in the field of composite fabrication by FSP has a great scope of exploring the possibility of processing harder materials by this technique in addition to the biological applications of the fabricated composites. Different reinforcements and substrate materials can be used and the process variables can also be optimized.

#### Acknowledgement

Authors acknowledge the Indian Institute of Technology Ropar, India for the lab equipment.

#### REFERENCES

- [1] S. Anbu selvan, S. Ramanathan, *Materials & Design* **31** (4), 1930-1936 (2010).
- [2] H. Arora, H. Singh, B. Dhindaw, *Wear* **303** (1), 65-77 (2013).
- [3] S. Alidokht, A. Abdollah-Zadeh, S. Soleymani, H. Assadi, *Materials & Design* **32** (5), 2727-2733 (2011).
- [4] H.Z. Ye, X.Y.J.J.o.m.s. Liu **39** (20), 6153-6171 (2004).
- [5] H.S. Arora, H. Singh, B.K. Dhindaw, *The International Journal of Advanced Manufacturing Technology* **61** (9-12), 1043-1055 (2011).
- [6] Z.Y.M. R.S. Mishra, I. Charit, *Materials Science and Engineering A* **341**, 307-310 (2003).
- [7] J. An, R. Li, Y. Lu, C. Chen, Y. Xu, X. Chen, L. Wang, *Wear* **265** (1), 97-104 (2008).
- [8] Y. Zhang, S. Yu, Y. Luo, H. Hu, *Materials Science and Engineering A* **472** (1-2), 59-65 (2008).
- [9] M. Habibnejad-Korayem, R. Mahmudi, H. Ghasemi, W. Poole, *Wear* **268** (3), 405-412 (2010).
- [10] A. López, P. Rodrigo, B. Torres, J. Rams, *Wear* **271** (11), 2836-2844 (2011).
- [11] H.S. Arora, H. Singh, B.K. Dhindaw, *Journal of Materials Engineering and Performance* **21** (11), 2328-2339 (2012).
- [12] I. Aathisugan, A.R. Rose, D.S. Jebadurai, *Journal of Magnesium and Alloys* **5** (1), 20-25 (2017).
- [13] O. Tinubu, S. Das, A. Dutt, J. Mogonye, V. Ageh, R. Xu, J. Forsdike, R. Mishra, T. Scharf, *Wear* **356**, 94-100 (2016).
- [14] Y. Huang, J. Li, L. Wan, X. Meng, Y. Xie, *Materials Science and Engineering A* **732**, 205-211 (2018).
- [15] N. Singh, J. Singh, B. Singh, N. Singh, *Materials Today: Proceedings* **5** (9), 19976-19984 (2018).
- [16] S. Arokiasamy, B.A.J.T.I.J.o.A.M.T. Ronald **93** (1-4), 493-503 (2017).
- [17] M. Dadashpour, A. Mostafapour, R. Yeşildal, S.J.M.S. Rouhi, E. A **655**, 379-387 (2016).
- [18] M. Azizieh, M. Mazaheri, Z. Balak, H. Kafashan, H.S.J.M.S. Kim, E. A, **712**, 655-662 (2018).
- [19] N. M., *International Journal of Modern Physics B* **22** (18 & 19), 2879-2885 (2008).
- [20] H.S. Arora, H. Singh, B.K. Dhindaw, *Wear* **303** (1-2), 65-77 (2013).